Journal of Nuclear Materials 390–391 (2009) 951–954

Contents lists available at ScienceDirect

Journal of Nuclear Materials

journal homepage: www.elsevier.com/locate/jnucmat

ICRF specific impurity sources and plasma sheaths in Alcator C-Mod

S.J. Wukitch *, B. LaBombard, Y. Lin, B. Lipschultz, E. Marmar, M.L. Reinke, D.G. Whyte, The Alcator C-Mod Team

MIT Plasma Science and Fusion Center, NW21-103, 190 Albany St., Cambridge, MA 02139, USA

ARTICLE INFO

PACS:
52.40.Fd
52.40.Hf
52.40.Kh
52.40.Qt

ABSTRACT

In Alcator C-Mod, we have sought to identify ICRF specific impurity sources and estimate the lifetime of thin, low-Z films in the presence of high power ICRF heating. With ICRF, the erosion rate of low-Z films is estimated to be 15–20 nm/s indicating the eroding species energy is much higher than that normally found in the SOL. Using emissive probes, plasma potential measurements confirm the presence of an enhanced sheath with ICRF when the probe is magnetically linked to the active antenna. Plasma potentials were typically 100–200 V for ~1.25 MW injected ICRF power. Furthermore, an RF sheath was unexpectedly present with insulating limiters and was dependent on the wall conditions and plasma confinement. These dependencies suggest that other scrape-off layer and plasma-surface characteristics are influencing the resulting RF sheaths.

1. Introduction

The primary role for ion cyclotron range of frequency (ICRF) power on ITER and future fusion reactors is to provide bulk plasma heating [1] where high Z metallic plasma facing components (PFCs) are being envisioned [2]. To inject ICRF power, the coupling antenna structure needs to be situated near the plasma edge and one of the primary ICRF utilization challenges is to reduce/eliminate ICRF specific impurity production. Previously a prescription to ameliorate impurity production was developed empirically for experiments with carbon plasma facing components (PFC) [3]. In next step devices including ITER, high-Z metallic PFCs for fusion are being considered despite obvious obstacles [2,4] including restrictive core tungsten concentration, $<10^{-5}$ [5]. Furthermore, increased impurity confinement is characteristic of H-mode and internal transport barriers suggesting that even minor impurity sources could be problematic for a burning plasma.

A generally accepted model for ICRF induced impurity production is enhanced sputtering caused by RF rectified sheaths (RF sheaths) with substantially higher sheath voltages than expected for thermal sheaths (~3–4 Te) [6]. Simply stated, RF sheaths form on open field line with its ends terminating on conducting surfaces enclosing an area where RF flux changes lead to voltage changes on the field line at the RF frequency. Electrons respond to the RF and are preferentially lost to conducting surfaces while ions are relatively immobile. To maintain ambipolarity, the plasma potential along the field line increases to reduce the electron losses. RF sheaths based on this model are often referred to as "near-field" RF sheaths which can be present both locally at antenna elements and to locations linked by a magnetic field line to the antenna [7]. From this model, the sheath voltage is expected to scale with the current in the antenna strap and can be related to the delivered RF power [8,9]. Another type of RF sheath has been identified as a far-field sheath [10,11]. Here, the RF sheath forms when the launched plasma wave has weak single pass absorption and the wave fields occupy the torus volume. The RF wave energy interacts directly with the sheath at the boundary and results in an enhanced sheath voltage and subsequent increase in sputtering. Far field sheaths are differentiated from near field in that they are not magnetically linked to the RF antenna and would increase impurity production at locations not magnetically linked to the antenna.

RF sheaths are important because the impurity influx resulting from ion sputtering at PFC surfaces is a sensitive function of the sheath potential. The impurity influx is proportional to the product of the effective yield (Y_{eff}) and ion flux to the material surface where Y_{eff} is a function of sheath voltage, see Fig. 1 [12]. We have assumed for a deuterium plasma that there are trace amounts of boron (1%) and molybdenum (0.1%) based on previous measurements and modeling of the divertor sputtering [13] and core plasma measurements [14]. For molybdenum PFCs, Y_{eff} is dominated by impurity sputtering below 100 V and increases rapidly for voltages above 100 V where deuterium sputtering dominates.

Despite the differences in geometric size between ITER (R = 6.2 m) and Alcator C-Mod (R = 0.67 m), C-Mod has characteristics that are similar to conditions expected in ITER. The C-Mod ICRF antennas can obtain power densities (10 MW/m^2) in excess of the ITER antennas. The RF wave single-pass absorption is similar; thus,

* Corresponding author.
E-mail address: wukitch@psfc.mit.edu (S.J. Wukitch).

0022-3115/$ - see front matter © 2009 Published by Elsevier B.V.
doi:10.1016/j.jnucmat.2009.01.245

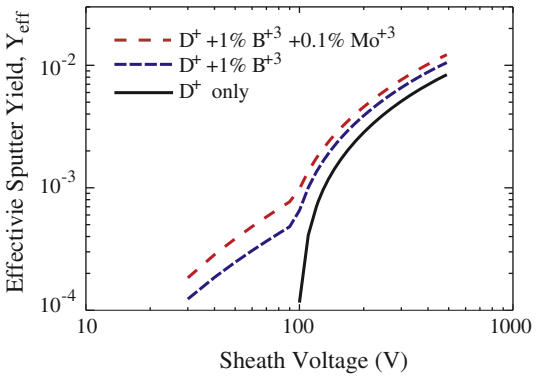

Fig. 1. Effective sputtering yield for deuterium on molybdenum, deuterium with 1% boron^{+3} on molybdenum, and deuterium with 1% boron^{+3} and 0.1% molybdenum^{+3} on molybdenum.

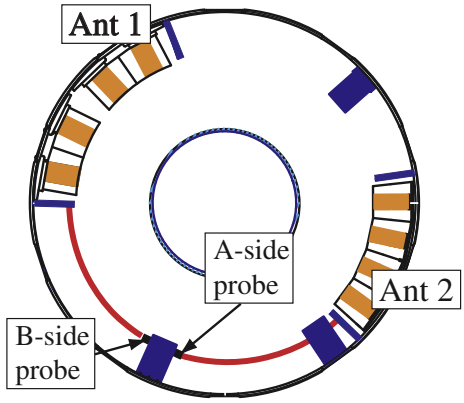

Fig. 2. Emissive probes are magnetically connected to the antenna limiter tiles. B-side probe is linked to Ant 1 near the top of the antenna and A-side probe is linked to Ant 2 near the bottom of that antenna. Note the field line passes under the local plasma limiter located near Ant 2.

the RF fields in C-Mod plasmas will be localized toroidally. Furthermore, C-Mod utilizes high-Z (molybdenum) PFCs. The scrape-off layer is also opaque to neutrals in C-Mod, an important consideration for impurity transport, as it is expected in ITER. In addition to the high Z PFCs being considered for ITER, beryllium has been proposed to cover most of the first wall and the ICRF faraday screen. In C-Mod, we can coat the PFCs with a low-Z boron film in situ [14], using the so-called 'boronization' technique allowing an opportunity to investigate the compatibility of high power ICRF and low-Z films. In the experiments described below, the primary goal was to identify the important impurity source locations. We also sought to characterize the plasma potential modifications associated with the ICRF to develop a better understanding of the underlying physics of ICRF-derived impurity generation.

2. Experimental setup

Alcator C-Mod is a compact (major radius $R = 0.67$ m, minor radius $a = 0.22$ m), high field ($B_T \leqslant 8.1$ T) diverted tokamak with molybdenum PFCs and auxiliary RF heating and current drive [15]. The discharges analyzed here are lower single-null, 1 MA deuterium discharges using hydrogen minority heating with the hydrogen cyclotron resonance near the magnetic axis, 5.2–5.4 T where the hydrogen concentration is typically 3–5% corresponding to strong single pass absorption. For these experiments, 2–3 MW of ICRF power is used to heat discharges with central density $\leqslant 2 \times 10^{20}$ m^{-3}. The ICRF power is coupled by two-strap D and E antennas, [16] operated in dipole $(0,\pi)$ phasing and are referred to as antenna 1, and the four-strap antenna, antenna 2, [17] is operated at 78 MHz in dipole phasing $(0,\pi,0,\pi)$. The local RF limiters at the antennas are ~1 cm radially behind the plasma limiters and can be armored with either molybdenum or boron nitride tiles. Two emissive probes are utilized to measure the plasma potential [13,18]. These probes consist of thin thoriated tungsten wire maintained at ~1800 C where the emitted electron current is greater than the free streaming electron flux. The floating potential of the heated filament is a measure of the plasma potential to with $\sim T_e$ [18]. The probes are on field lines that connect the RF antenna and plasma limiter and are shown schematically in Fig. 2. The A-side probe maps to antenna 2 below the mid-plane near the antenna top corner and the B-side probe is linked magnetically to the antenna 1 above the mid-plane near the antenna bottom corner. Both probes are linked to regions where the RF sheath is expected to be significant [9,19,20].

Utilizing an electron cyclotron resonance discharge (ECDC), a thin film of boron is deposited on the PFCs, so-called boronization, with the boronization plasma characteristics have been reported elsewhere [14]. Boron deposition is limited to the radial region where the boronization plasma density is significant, a region is bounded by the cyclotron resonance on the inboard side and the upper hybrid resonance on the outboard where the radial separation between the two resonances is typically ~7–8 cm. For the experiments described herein, a thin film (15–20 nm) is applied by sweeping the ECDC resonance location between 0.65 m and 0.75 m for 10 min.

3. Experimental results

Previous experiments had shown that the core molybdenum content and molybdenum source rate at the active antenna increased with ICRF power and RF sheaths up to 400 V were observed on flux tubes connected to the antenna [13]. In an effort to eliminate the local molybdenum impurity source and eliminate the RF-derived sheaths we replaced the molybdenum tiles with insulating boron nitride (BN) tiles on all antennas. The insulating tiles effectively act as additional impedance on the flux tube; thus flux tubes not intercepted by the BN tile would be unaffected. If BN tile impedance is sufficiently higher than the sheath impedance then the potential drop imposed by RF should fall across the insulator rather than the plasma-PFC sheath [21]. The tiles are 3.175 cm thick and BN has a relative permittivity of four. Following reference [21] and using typical measured sheath voltages with metallic limiters, the impedance of the BN tiles (~1.7 ohm m^2) is expected to be ~100× the sheath impedance (~0.005 ohm m^2). Surprisingly, the plasma performance and core Mo content were unimproved with the BN RF limiter tiles.

Since RF sheaths are expected to be important, we sought to characterize the RF sheaths through measurements of the plasma potential using emissive probes. Measurements confirmed that the plasma potential responds primarily when the probe is magnetically linked to the active antenna [13]. In the following discussion, all the results correspond to B-side emissive probe which is linked to Antenna 1 due to the larger available data base. In Fig. 3, the scaling of the plasma potential with RF power is shown for discharges following a boronization and those without recent boronization. At the highest power level, the plasma potential can be 100–150 V for the latter case while ~60 V just following boronization. Furthermore, the plasma potential scales as the square root of the RF power for the boronized case whereas in the case without recent boronization the voltage scales linearly with power.

There are also differences in RF-induced sheaths between L-mode and H-mode discharges. In Fig. 4 we show a comparison of

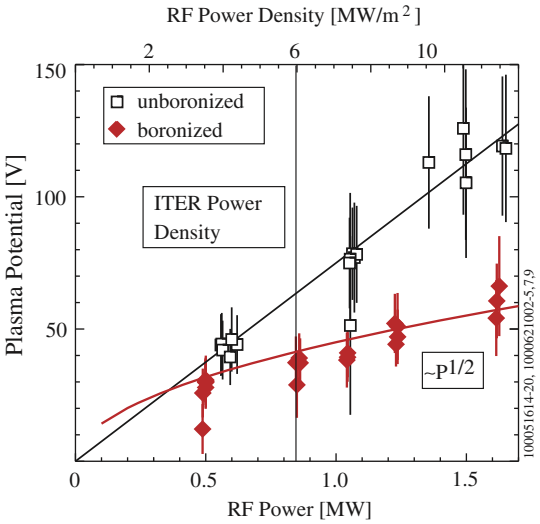

Fig. 3. In L-mode discharges, the measured plasma potential scales as the square root of the RF power for recently boronized PFCs and linear with RF power for unboronized PFCs.

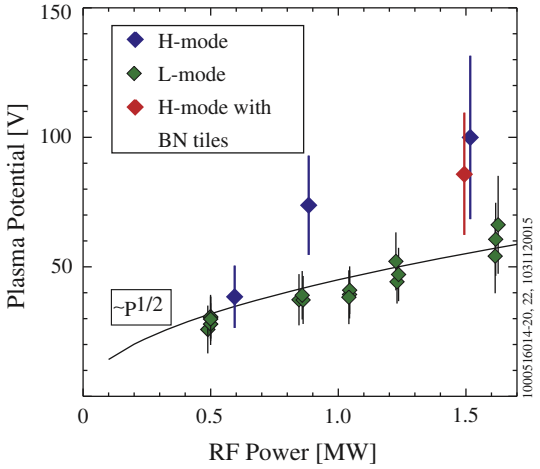

Fig. 4. Comparison of the measured plasma potential for L and H-mode discharges showing that the H-mode potential is ~2× L-mode. Comparing an H-mode discharge with BN tiles, shows the RF sheath is unaffected relative to the RF sheath in H-mode with metallic RF limiter tiles.

L and H-mode data from separate discharges. Here, the H-mode plasma potentials are higher than the L-mode case by about a factor of 2. Furthermore, the measured plasma potential was essentially the same with BN tiles as with Mo tiles.

4. Discussion

From previous experiments [16], a source outside the divertor appeared to be the primary contributor to the core Mo and the expectation was that the antenna limiters would be the dominant contributors. Experiments optimizing the plasma performance through radial localized boronization suggested the top of the outer divertor and plasma limiter as potential source locations. Mapping the connection of the antennas along field lines to different Mo tile locations and the experiments linking the erosion and impurity production to the active antenna are consistent with this hypothesis [22]. The results from operation with insulating RF limiters on all antennas are consistent with the hypothesis that additional impurity sources away from the antenna are important.

These experiments also gave an estimate of the erosion rate of low-Z materials by RF sheaths. The estimated boron film thickness is 15–20 nm for the between discharge boronization and we observe that this layer is removed in a single discharge using ~3 MW of ICRF power for ~1 s. The estimated erosion rate is thus 15–20 nm/s. We note that in the original beryllium experiments on JET that significant beryllium influx was observed but the erosion rate was not estimated [23]. Assuming a similar erosion rate for beryllium in ITER as the B erosion rate in C-Mod, the number of discharges to erode through 1 cm of a beryllium tile is ~1000 discharges (400 s discharges). Thus, any low-Z-film or even bulk PFC is likely to have a relatively short lifetime in the presence of RF sheaths.

Based on Phaedrus-T experiments [24] and the RF sheath model, we expected that switching the antenna limiter tiles to BN would eliminated the primary Mo source affecting the plasma. However, the C-Mod data clearly indicates the presence of RF sheaths despite thick BN tiles on the RF limiter. One possible explanation is that the RF sheath model needs to allow for cross-field currents [25,26]. In such a case ion flows across the magnetic field along the length of the flux tube between antenna and main limiters and would be balanced by electron currents in and out of one end of the flux tube still connected to Mo tiles. This would require the impedance integrated along the flux tube to be less than or equal to the impedance through the sheath. Another possibility is the development of an energetic edge electron population. We note that relatively small energetic electron population, ~0.1% can double the sheath voltage and a population of a few percent can increase the sheath potential by a factor of 10 [27]. A number of mechanisms have been proposed, two of which are Fermi acceleration [28] and near field acceleration similar to that observed with lower hybrid couplers [29]. Both mechanisms would create electrons on field lines linked to the active antenna and might not have been dominant in the Phaedrus-T experiment because of the low power, 10–40 times less than C-Mod's, used in those experiments.

The RF sheath model predicts that the RF sheath voltage should scale as the square root of the RF power [8]. For the recently boronized case, the plasma potential follows the predicted trend. However, when the B layer is eroded, the plasma potential scales with the RF power. This suggests that the induced plasma potential can be influenced by factors other than the RF voltage. Another possible explanation is that the local density profile is changing with RF power and complicating the scaling. Although direct measure of the density profile is lacking, the antenna load gives an indirect measure of the profile because of the sensitivity to the density profile. In these power ramps, the antenna loading is constant above 100 kW.

Another indication that other factors can influence the RF sheath voltage is the increased RF sheath in H-mode compared to L-mode. If one assumes that the surface conditions were held constant across a transition from L and H-mode, one would expect that the induced sheath voltages would increase with the current in the antenna strap based on the RF sheath model. From current probes in the antenna and measurements of the antenna resistance, the RF sheath voltage was expected to increase by ~20% for the case shown in Fig. 4, but the observed RF sheath voltage nearly doubled. This further indicates the RF sheath voltage per applied RF voltage is strongly dependent on other factors. For sake of discussion, assume the RF sheath voltage is set by an edge energetic electron population. In the case of H-mode, the edge collisionality is lower than in L-mode; thus, the electron population can be more energetic and a larger fraction of the total electron population. This would lead to larger RF sheath voltages in the H-mode case compared to the L-mode regime.

These observations require more detailed experimental investigation to further understand the origin and behavior of the RF

sheaths. The diagnostic array should include emissive probes with complementary magnetic probes to measure RF wave fields and retarding energy analyzers to measure the electron distribution. Additional important diagnostics would include spectroscopic determination of the local impurity source rate where the RF sheath voltage is measured and a scrape-off layer reflectometer to measure the local density profile at the antenna. In addition to diagnostics, a more complete investigation of the RF sheath parametric dependence on plasma density, current and majority species could provide some insight on the important plasma parameters. In addition the influence of strength of wave absorption could also be an important issue.

Acknowledgements

We greatly appreciate the efforts of the entire Alcator C-Mod physics and operational staff. This work is supported by US Department of Energy Coop. Agreement DE-FC02-99ER54512.

References

[1] ITER Physics Expert Group, Nucl. Fus. 39 (1999) 2495
[2] F. Najmabadi, The ARIES Team, Fus. Eng. Des. 80 (2006) 3.
[3] J. Jacquinot et al., Fus. Eng. Des. 12 (1990) 245.
[4] H. Bolt et al., J. Nucl. Mater. (2002) 435;
M. Gasparotto et al., Fusion Engineering and Design 66-68 (2003) 129;
H. Bolt et al., J. Nucl. Mater. 329-222 (2004) 66;
F. Najmabadi, The ARIES Team, Fus. Eng. Des. 80 (2006) 3.
[5] R.V. Jensen, D. E Post, D.L. Jassby, Nucl. Sci Eng. 65 (1978) 282.
[6] J. Myra, in: 16th Topical Conference on RF Power in Plasmas, AIP Conference Proceedings, vol. 787, 2006, p. 3;
J. Myra et al., Nucl. Fus. 46 (2006) S455.
[7] C.E. Thomas et al., Fus. Technol. 30 (1996) 1.
[8] J.R. Myra et al., Fus. Eng. Des. 31 (1996) 291.
[9] D.A. D'Ippolito et al., Nucl. Fus. 38 (1998) 1543.
[10] M. Brambilla et al., in: Proceedings of the 13th IAEA Conference on Plasma Physics and Controlled Nuclear Fusion Research, IAEA (Vienna), Washington, 1990, p. 723.
[11] J.R. Myra, D.A. D'Ippolito, Phys. Plasmas 1 (1994) 2890.
[12] W. Eckstein, J. Bohdansky, J. Roth, Nucl. Fus. 1 (1991) 51.
[13] B. Lipschultz et al., Nucl. Fus. 41 (2001) 585.
[14] B. Lipschultz et al., Phys. Plasmas 13 (2006) 056117.
[15] I.H. Hutchinson et al., Phys. Plasmas 1 (1994) 1511.
[16] Y. Takase, S.N. Golovato, M. Porkolab, K. Bajwa, H. Becker, D. Caldwell, in: 14th Symposium on Fusion Eng., IEEE, San Diego, 1992, Piscataway, NJ, p. 118.
[17] S.J. Wukitch, R.L. Boivin, P.T. Bonoli, et al., Plasma Phys. Control. Fus. 46 (2004) 1479.
[18] E.Y. Wang et al., J. Appl. Phys. 61 (1987) 4786.
[19] D.A. Diebold et al., Nucl. Fus. 32 (1992) 2040.
[20] L. Colas et al., Plasma Phys. Control. Fus. 49 (2007) B35.
[21] J.R. Myra, D.A. D'Ippolito, J.A. Rice, C.S. Hazelton, J. Nucl. Mater. 249 (1997) 190.
[22] S.J. Wukitch et al., J. Nucl. Mater. 363-365 (2007) 491.
[23] M. Bures, J. Jacquinot, M. Stamp, K. Lawson, P. Thomas, Fus. Eng. Des. 12 (1990) 251.
[24] J. Sorensen, D.A. Diebold, R. Majeski, N. Hershdowitz, Nucl. Fus. 33 (1993) 915;
J. Sorensen, D.A. Diebold, R. Majeski, N. Hershdowitz, Nucl. Fus. 36 (1996) 173.
[25] D.A.D. Ippolito et al., Nucl. Fus. 42 (2002) 1357.
[26] E. Faudot et al., Phys. Plasmas 13 (2006) 042512.
[27] D. Tskhakaya Jr, S. Kuhn, V. Petržílka, R. Khanal, Phys. Plasmas 9 (2002) 2486.
[28] M.D. Carter, D.B. Batchelor, E.F. Jaeger, Phys. Fluid B 4 (1992) 1081.
[29] V. Petržílka et al., in: Proceedings of the 32nd EPS Conference on Plasma Physics, vol. 29C, 2005, p. P-2.095.